Microchim Acta
DOI 10.1007/s00604-015-1660-z

ORIGINAL PAPER

Screening for cystic fibrosis via a magnetic and microfluidic immunoassay format with electrochemical detection using a copper nanoparticle-modified gold electrode

Maria Luz Scala Benuzzi[1] · **Sirley V. Pereira**[1] · **Julio Raba**[1] · **Germán A. Messina**[1]

Received: 30 July 2015 / Accepted: 7 October 2015

Abstract This article describes a microfluidic electrochemical immunoassay that features two strategies, viz. (a), the incorporation of magnetic nanoparticles (MNPs) into the central microfluidic channel and acting as a bioaffinity support for the immobilization of the antibody against the immunoreactive trypsin (anti-IRT), and (b), the electrodeposition of copper nanoparticles (CuNPs) on a gold electrode. IRT, a marker for cystic fibrosis, is extracted from blood samples onto a disk using ultrasonication, eluted, and then injected into the detection system where it is captured by anti-IRT-loaded nanoparticles (anti-IRT-Ab-MNPs). Bound IRT is electrochemically quantified after addition of HRP-labeled anti-IRT-Ab which, in the presence of H_2O_2, catalyzes the oxidation of catechol to form o-benzoquinone which is detected at a working potential of −150 mV (vs. Ag/AgCl). The electrochemical response to benzoquinone is proportional to the concentration of IRT in the range from 0 to 580 ng·mL^{-1}. The coefficients of variation are <5 % for within-day assays, and <6.4 % for between-day assays. The method was compared to a commercial ELISA for IRT where is showed a correlation coefficient of close to 1. In our perception, this approach represents an attractive alternative to existing methods for screening newborns for cystic fibrosis.

Keywords Immunoassay · Amperometry · Cyclic voltammetry · Horse radish peroxidase · Immunoreactive trypsin · Magnetic nanoparticles · Hydrogen peroxide · Electrodeposition

Introduction

Cystic Fibrosis (CF) is an autosomal-recessive disorder caused by mutations in the CF transmembrane conductance regulator (CFTR) gene [1]. CF generates a multi-organ pathology clinically characterized by lung disease (chronic infection, inflammation, and airways obstruction), gastrointestinal abnormalities (pancreatic insufficiency, malabsorption, and malnutrition), salt loss (high sweat electrolytes), and other manifestations (intestinal obstruction, cirrhosis, diabetes, etc.) [2].

CF has no cure [3], consequently an early and adequate diagnosis is essential to start the treatment as early as possible to prevent malnutrition and irreversible lung damage [4]. In order to achieve this goal, Newborn Screening (NBS) for CF has been implemented as a public health strategy. The increased immunoreactive trypsin (IRT) level during the first month of life represents the primary biomarker of CF newborn screening. For this reason, all CF screening programs rely on measurement of IRT from a dried blood sample taken during the first week of newborn's life [5]. The IRT cutoff value in most of countries ranges between 60 and 70 ng mL^{-1} [6–8].

Analytical methods employing high performance liquid chromatography (HPLC), mass spectrometry (MS), LC–MS/MS, and gas chromatography–mass spectrometry (GC–MS) are being developed for newborn screening [9–12]. Although, these techniques may provide efficient determination, they are laborious, time-consuming, require large volume of sample and expensive equipment.

Electronic supplementary material The online version of this article (doi:10.1007/s00604-015-1660-z) contains supplementary material, which is available to authorized users.

✉ Germán A. Messina
messina@unsl.edu.ar

[1] INQUISAL, Department of Chemistry, National University of San Luis, CONICET, Chacabuco 917. D5700BWS, San Luis, Argentina

Published online: 19 October 2015

Alternatively, immunosensors applied to the diagnostic of newborn diseases are being considered as an attractive choice, because of their intrinsic advantages, such as high sensitivity, good specificity and less dependence on sample pretreatment [13]. Moreover immunoassay can be performed in a microfluidic platform. Microfluidic technology allowed the miniaturization of devices, which results in a substantial reduction of reactive solutions, shorter analysis time, improved portability [14], and better detection limits (LODs) [15].

The electrochemical detection coupled to microfluidic sensors has received considerable attention due to their inherent simplicity, compatibility with microfabrication techniques, high sensitivity, fast detection, and low cost [16].

Microfluidic platforms allow performing electrochemical immunoassays employing nanomaterials. In recent years there has been an intensive research into the development of a variety of inorganic, organic, polymeric and biological nanomaterials for biomedical applications [17, 18]. Among them, Nanoparticles (NPs) have often been introduced within microfluidics system due to they have unique properties such as large surface area, high bioaffinity and excellent stability [19]. Introducing nanoparticles as support of immunoreagents provides a large availability of binding sites. Particularly, magnetic nanoparticles (MNPs) provide an extra advantage in their manipulation and detection (e.g. stirring, positioning recuperation and sensing), which can be easily performed with the aid of an external magnetic field [20].

Moreover, the incorporation of nanomaterials on electrode surface provides many benefits for electrochemical detection in microfluidic sensors [21]. Nanomaterial-based electrode offer many advantages over conventional ones better stability, greater sensitivity, lower detection limits, lowering of detection potentials via electrocatalytic effect or lowering of current densities at the electrode surface [22].

The nanomaterials deposition on electrode surface is being performed via a variety of strategies, such as the impregnation of metal precursors followed by chemical or physical reduction [23], sol–gel derived process [24], electrodeposition [25], and electroless deposition [26]. The electrodeposition represents a simple and versatile tool for biosensors fabrication, which exhibited good stability, reproducibility and short response time [27]. It is a kinetic-controlled process involving preferential nucleation and subsequent growth of metal NPs on an appropriate electrode surface [28].

Different electrodes modified with metallic nanoparticles such as platinum [29], silver [30], and gold [31] have been reported. Although improved performance was described, the high cost and the limited availability of some of these materials can impose restrictions to the development of inexpensive sensors. Electrodeposited copper NPs (CuNPs) represent an alternative material with potential applications in medicine [32]. The use of CuNPs on electrodes surface is an interesting strategy to achieve the electrode modification and consequently the improvement of electrochemical detection [33].Despite their potential toxicity [34], CuNPs are less expensive and provide access to a number of chemical routes for their derivatization. Their reactivity and molecular recognition capabilities have also sparked their use in electrochemical biosensors [35].

In the present work, a microfluidic immunosensor with electrochemical detection has been developed in order to quantify IRT in blood spot samples. For this purpose, anti-IRT-Ab was immobilized onto MNPs surface, which were retained in the central channel of the device. The antibody recognized specifically the IRT present in samples. The detection was achieved by adding HRP-conjugated anti-IRT-Ab using catechol (Q) as enzymatic mediator. HRP in the presence of hydrogen peroxide (H_2O_2) catalyzed the oxidation of Q to o-benzoquinone (P). The subsequently reduction was performed by a gold electrode with electrodeposited CuNPs at −150 mV. The response current obtained from the product of the enzymatic reaction was proportional to the activity of the enzyme and consequently, to the IRT present in samples.

Materials and methods

Reagents and solutions

Soda lime glass wafers (26 × 76 × 1 mm) were purchased from Glass Técnica (São Paulo, Brazil). Sylgard 184 and AZ4330 photoresist (PR) were obtained from Dow Corning (Midland, MI, USA www.dowcorning.com) and Clariant (Sommerville, NJ, USA www.clariant.com), respectively. Carboxi-functionalized magnetic nanoparticles, Hydrofluoric acid (HF), N-hydroxysuccinimide (NHS), 1-ethyl-3-(3-dimethylaminopropyl)carbodiimide (EDC) and 3-aminopropyl triethoxysilane (APTES) were purchased from Sigma–Aldrich (Argentina, www.sigmaaldrich.com). Hydrogen peroxide (H_2O_2) and catechol were purchased from Merck (Argentina, www.merck.com.ar). ImmunoChem Blood Spot Trypsin-MW ELISA (enzyme-linked immunosorbent assay) Kit (MP Biomedicals, USA), was purchased from Laboratorios Bacon (Argentina, www.bacon.com.ar) and used according to the manufacturer's instructions [36]. Anti-IRT–mouse monoclonal antibody (anti-IRT-Ab) and horseradish peroxidase (HRP)-conjugated anti-IRT–Ab were purchased from Abcam (USA, www.abcam.com).

Instrumentation

Electrochemical measurements were performed using BAS 100B (electrochemical analyzer Bioanalytical Systems West Lafayette, IN, USA www.basinc.com). A three electrode system were used, where a gold (Au) electrode, a platinum electrode and a Ag/AgCl wire served as a working, auxiliary and reference electrode, respectively.

Amperometric measurements were performed using the biosensor developed tandem BAS LC 4 C (Bioanalytical Systems, West Lafayette, IN, USA www.basinc.com).The syringe pump system (Baby Bee Syringe Pump, Bioanalytical Systems) was used to pumping and stopping flow. The morphologies of the CuNPs electrodeposited onto Au electrode were studied by LEO 1450VP scanning electron microscope (SEM). An energy dispersive X-ray spectroscopy (EDS) with a LEO 1450VP scanning electron microscope was used to analyze the elemental composition of the electrode. Absorbance was detected using a BIOTEK Epoch microplate reader and a Beckman DU 520 general UV/VIS spectrophotometer.

Microchip fabrication

The construction was carried out according to the procedure described in Ref. [37] with the following modifications. The device layout was drawn using CorelDraw software version 11.0 (Corel) and printed on a high-resolution transparency film in a local graphic service, which was used as a mask in the photolithographic step. The microfluidic chip design consisted of a T-type format. The lengths of the central and accessory channels were 15 and 60 mm, respectively. The printed transparency mask was placed on top of a glass wafer previously coated with a 5 μm layer of AZ4330 PR. The substrate was exposed to UV radiation for 30 s and developed in AZ 400 K developer solution for 2 min. Glass channels were etched with an etching solution of 20 % HF for 4 min under continuous stirring (check the HF material safety data sheet). The etching rate was 8 ± 1 μm min^{-1}. Following the etching step, substrates were rinsed with deionized water and the PR was removed with acetone. To access the microfluidic network, holes were drilled on glass-etched channels with a Dremel tool (MultiPro 395JU model, USA) using 1-mm diamond drill bits.

To achieve the final chip format, another glass plate was spincoated with a thin poly(dimethylsiloxane) (PDMS) layer at 3000 rpm for 10 s. PDMS was prepared with a 10:1 mixture of Sylgard 184 elastomer and a curing agent. The thickness of this layer was 50 μm. Before sealing, the PDMS layer was cured at 100 °C for 5 min on a hot plate. Glass channels and PDMS-coated glass substrate were placed in an oxygen plasma cleaner (Plasma Technology PLAB SE80 plasma cleaner) and oxidized for 1 min. The two pieces were brought into contact immediately after the plasma treatment, obtaining a strong and irreversible sealing. The final device format was achieved in less than 30 min. The bonding resistance of the device was evaluated under different pressure values by using a high-performance liquid chromatography (HPLC) pump. The flow rate ranged from 10 to 300 μL min^{-1}.

Covalent binding of anti-IRT antibody onto MNPs

Magnetic particle modification was carried out using a carbodiimide/succinimide reaction. 100 μL of MNPs, previously washed with phosphate buffered saline solution (0.01 M, pH 7.2) (PBS), were suspended in 1 mL of solution 0.05 M (pH 7.2) of EDC and NHS with continuous stirring during 3 h at room temperature. Later, they were washed and incubated with a solution of 10 μg ml^{-1} anti-IRT–Ab in PBS during 12 h at 5 °C, with continuous stirring. Finally, the MNPs with anti-IRT-Ab immobilized (anti-IRT–Ab-MNPs) were washed and resuspended in 250 μL PBS solution at 5 °C. This preparation was stable for at least 1 month.

Gold electrode surface modification

With the purpose to obtain an improvement in the signal response, CuNPs electrodeposition onto Au electrode (CuNPs-AuE) surface was carried out.

The surface of a gold electrode must be cleaned previously to the electrodeposition process. The sulfuric acid potential cycling is a very common electrochemical cleaning technique [38]. According to this cleaning procedure, the AuE in the central channel of the microfluidic system was exposed to 0.05 M H_2SO_4 solution, performing potential cycles in the range 0.0–1.5 V, with a scanning rate of 0.1 V s^{-1} until reproducible cyclic voltammograms were obtained.

In order to achieve the electrode modification, a solution 0.1 M H_2SO_4 + 1 mM $CuSO_4$ was pumped at a flow rate of 2.0 μL min^{-1} during 3 min, while a − 500 mV potential was applied. After this modification, the electrode surface was characterized by SEM and EDS.

Sample preparation

Neonatal samples and control samples were provided by the Blood Spot Trypsin-MW ELISA Kit were used. The Kit specifies how these samples were obtained: blood samples were spotted in filter paper number 903 in the center of a 1 cm circle and allowed to diffuse outward, trying to avoid tearing or disrupting the filter paper surface. The specimens were allowed to air dry completely (overnight), avoiding heat, direct sunlight, and absorbent surfaces. After drying overnight, these were stored in an airtight plastic envelope at less than −15 °C until assay.

In order to perform the IRT extraction, a disk was cut (punched) from a blood spot sample. Then, it was placed into an Eppendorf tube with 200 μL of PBS (0.01 M, pH 7.2) and exposed to a sonication procedure for 2 min following the procedure described by Seia et al. [39]. The content of all tubes was aspirated and the eluted samples were stored at 4 °C until use.

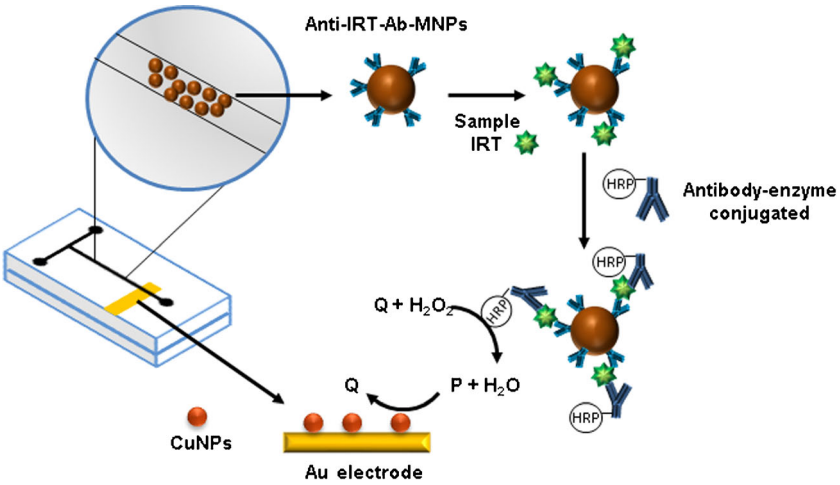

Scheme 1 Schematic representation of immunoreaction in the microfluidic device showing CuNPs electrodeposited on work electrode and the central channel incorporating anti-IRT-Ab-MNPs as bioaffinity support for the immune reaction

IRT determination

In order to avoid unspecific bindings, before performing the determination, anti-IRT–Ab-MNPs were exposed to a blocking treatment using 1 % of bovine serum albumin (BSA) in 0.01 M PBS (pH 7.2) for 5 min. After that, MNPs were washed 3 times with PBS, injected during 10 min into the central channel of the microchip and retained with an external magnet (supplementary data).

After each reagent solution injection, the central channel of the device was exposed to a washing procedure with PBS for 3 min to remove the reagent excess. All reagent solutions and samples were pumped at 2 μL min^{-1}.

The eluted sample was injected during 5 min and IRT was specifically recognized by the immobilized antibody. Later, bound IRT was quantified through the action of HRP-conjugated anti-IRT–Ab (dilution of 1:1000 in 0.01 M PBS, pH 7.2), which was injected for 5 min.

Finally, for the electrochemical detection, the substrate solution containing 0.001 M H_2O_2 and 0.001 M Q in 0.1 M phosphate–citrate buffer (pH 5.0) (supplementary data), was injected for 1 min. The enzymatic reaction product was detected through applying a − 150 mV potential (Scheme 1). Table 1 summarizes the complete analytical procedure.

Results and discussion

Characterization of the electrode surface

The morphology of CuNPs-AuE surface was studied by SEM. The Fig. 1 show unmodified AuE (1a) and CuNPs-AuE (1b), respectively. The diameter of the NPs was in a range of 50 nm. The elemental composition of the electrode surface was analyzed by EDS, the spectrum obtained shows the peaks corresponding to Au (at 2.12 and 9.71 keV) and Cu (at 0.93 and 8.04 keV) (1c).

The electrochemical characterization (1d) was carried out by Cyclic Voltammetry, monitoring a $Fe(CN)_6^{4-/3-}$ solution (1 mM $K_4[Fe(CN)_6]/K_3[Fe(CN)_6]$ in 0.1 M KCl (pH 6.50)). The potential scanning was performed from −250 to 500 mV vs. Ag/AgCl. The voltammograms obtained for the unmodified AuE (*i*) and CuNPs-AuE (*ii*) show that CuNPs increases the current peaks of $Fe(CN)_6^{4-/3-}$ solution.

Table 1 Summary of optimum conditions for IRT immunoassay

Sequence	Conditions	Time (min)
Blocking procedure	1 % of bovine serum albumin (BSA) in 0.01 M PBS (pH 7.2)	5
Washing step	(PBS, pH 7,2)	3
Injection of particles	Flow rate: 2,0 μL min^{-1} (PBS, pH 7,2)	10
Samples	Eluted sample flow rate of 2.0 μL min^{-1}	5
Washing buffer	Flow rate: 2,0 μL min^{-1} (PBS, pH 7,2)	3
Enzymatic conjugated	HRP-conjugated (dilution of 1/1000), 2,0 μL min-1	5
Washing buffer	Flow rate: 2,0 μL min^{-1} (PBS, pH 7,2)	3
Substrate	0.001 M H_2O_2 and 0.001 M Q (0.1 M phosphate–citrate buffer, pH 5.0)	1
Amperometric detection	Applied potential: -150 mV	1

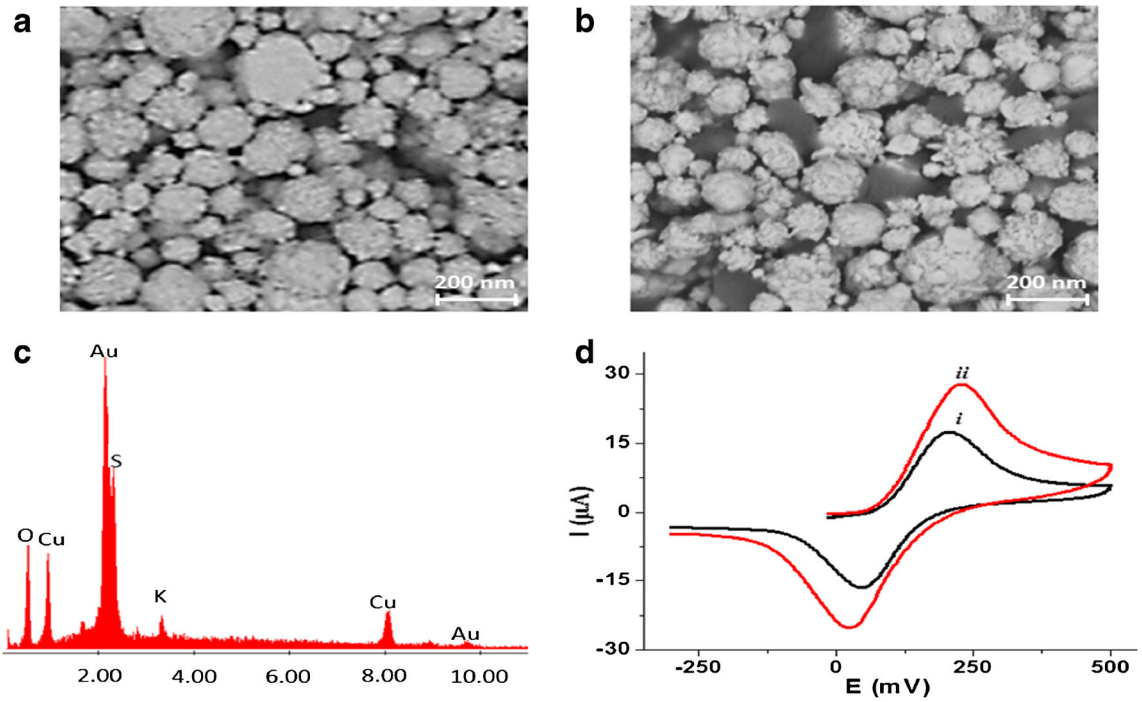

Fig. 1 Morphology characterization. The morphologies of unmodified AuE **a** and CuNPs-AuE **b** were investigated by SEM. The elemental composition of CuNPs-AuE was determined by EDS. **c**. Electrochemical characterization **d** of unmodified AuE (i) and CuNPs-AuE (ii) Cyclic Voltammetry was performed monitoring a $Fe(CN)_6^{4-/3-}$ solution (1 mM $K_4[Fe(CN)_6]/K_3[Fe(CN)_6]$ in 0.1 M KCl (pH 6.50)) from −250 to +500 mV at a scan rate of 50 mV s^{-1}

Electrochemical study of catechol on AuE

The study of catechol behavior on AuE was carried out by Cyclic Voltammetry. A Q solution in 0.1 M phosphate–citrate buffer (pH 5.0) was evaluated scanning in the potential range of −200 to 550 mV. The cyclic voltammograms obtained showed a good definition of the anodic and cationic peaks, which correspond to the transformation of Q to o-benzoquinone and vice versa. This is a quasi-reversible procedure in which 2 electrons are transferred. The relation of the current peaks, close to one, particularly when a repetitive cycling was performed, can be inferred as a stability criterion of the Q produced on the electrode surface in the work conditions employed (Data not shown).

Electrodeposition time and potential

The time and potential are relevant parameters in the electrodeposition process. For this reason, both parameters have been optimized. The electrodeposition time (tedep) was evaluated from 30 s to 180 s at −250 and −500 mV working electrode potential. The current intensity increased when the time grows until a value of 180 s, then the current remained constant. Therefore, a tedep of 180 s was selected as optimum.

The optimization of electrodeposition potential (Eedep) was performed using −250 and −500 mV as working electrode potential. The current increased by increasing the potential up to a value of −500 mV. Therefore, an Eedep of −500 mV was selected (Fig. 2).

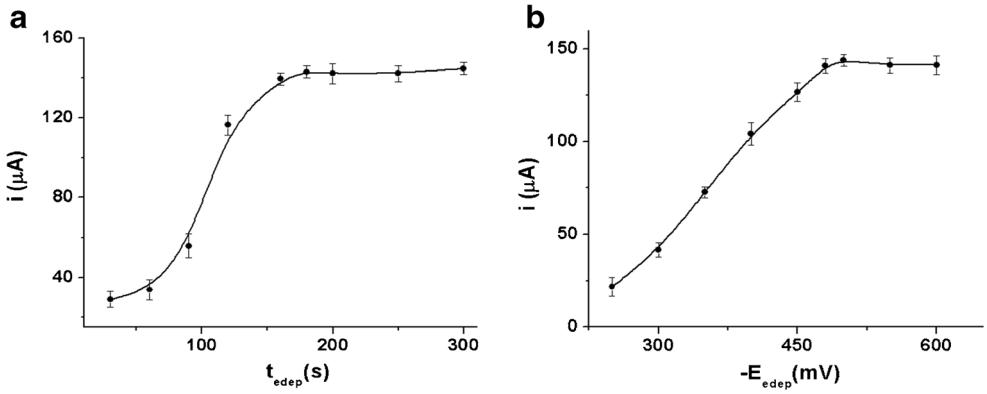

Fig. 2 **a** Effect of electrodeposition time employing a standard of 282 ng mL^{-1} and a Eedep 500 mV from 30 to 300 s. **b** Effect of electrodeposition potential employing a tedep 180 s from −250 to −600 mV

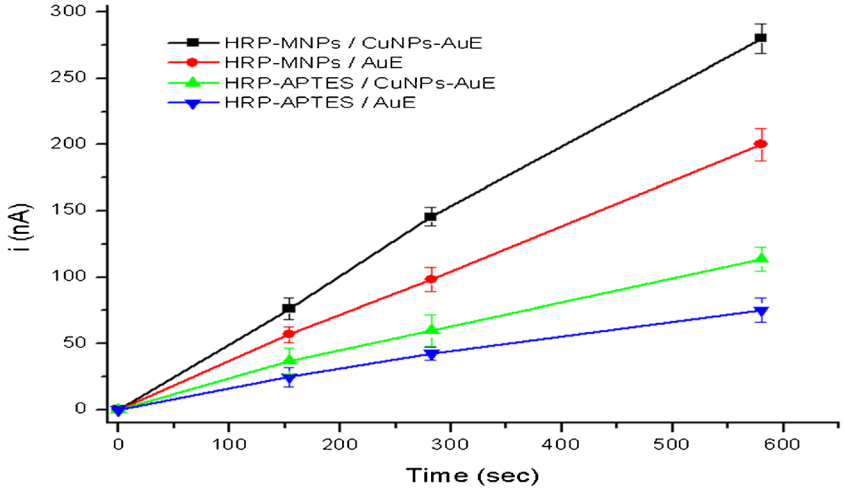

Fig. 3 Obtained signal intensity using HRP as indicator model. This figure compares the signal of the sensor incorporating HRP-MNPs and CuNPs-AuE **a**, the sensor incorporating HRP-MNPs and unmodified AuE **b**, the sensor with a central channel modified with HRP-APTES and CuNPs-AuE **c**, the sensor with a central channel modified with HRP-APTES with unmodified AuE **d**. For this study, 0.1 M phosphate–citrate buffer, pH 5.0, containing 0.001 M H_2O_2 and 0.001 M Q were injected at 2 μL min^{-1}, and the enzymatic product was measured by amperometry at −150 mV

Parameter optimization

The following parameters were optimized: (a) flow rate; (b) antibody concentration; (c) sample volume, Temperature and pH; (d) reaction time. Respective data and Figures are given in the Electronic Supporting Material. The following experimental conditions were found to give best results: (a) an anti-IRT-Ab concentration of. 10 μg mL-1 (b) a flow rate of 2 μL min-1, (c) a sample volume of 10 μL, an optimal temperature range of 20–25 °C and a pH value of 5.05 (d) an optimal reaction time of 5 min.

Amplification effect of the obtained signal

With the purpose of evaluate the amplification effect resulting from the incorporation of the MNPs, the signal intensity obtained using the sensor was compared with a signal obtained from a similar sensor in which the immunoreagents were incorporated by a direct modification of the central channel with –APTES (supplementary data). The Fig. 3 shows the signal amplification corresponding to the incorporation of MNPs into the central channel and the electrodeposited CuNPs-AuE.

Table 2 Within-assay precision (five measurements in the same run for each IRT control sample) and between-assay precision (five measurements for each IRT control sample, repeated for three consecutive days)

Standard[a]	Within-assay		Between-assay	
	Mean[a]	CV %	Mean[a]	CV %
53 ng mL^{-1}	53,61	3,23	53,97	4,85
154 ng mL^{-1}	153,32	3,88	152,32	6,35
580 ng mL^{-1}	581,71	4,98	587,02	5,12

[a] IRT concentration (ng mL^{-1})

Quantitative determination of IRT

If the electrochemical response of the enzymatic product was proportional to IRT concentration in samples was evaluated. The IRT calibration plot was obtained by plotting current (i) versus IRT concentration in the range of 0–580 ng mL^{-1}. The linear regression equation obtained was $i = 1.266 + 0.497$ x C_{TIR}. The correlation coefficient (r) for this plot was 0.998.

The precision of the method was checked with IRT samples at 53, 154, and 580 ng mL^{-1} concentrations. In order to estimate the precision, this assay was repeated 5 times a day and the series of analyses was repeated 3 consecutive days. The IRT assay showed a coefficient of variation (CV) within-assay values that were below 4.98 %, and the CV between-assay values were below 6.35 % (Table 2).

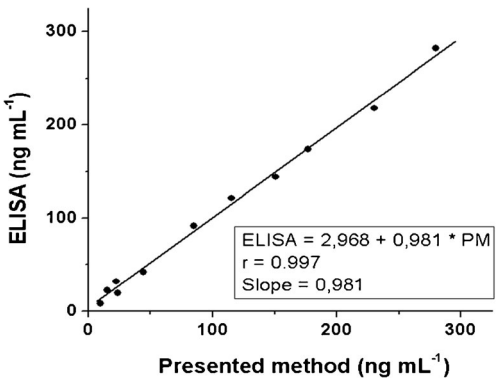

Fig. 4 Correlation between presented method and trypsin MW ELISA Kit. PM, presented method

Table 3 Comparison of electrochemical immunosensor with previously reported methods for the IRT determination

Detection system	Immunoassay format	Materials and applications	Linear range	LOD	Ref.
Fluorescence	Multiplexed immunoassay	-Luminex microespheres as immobilization support	0–1200 μg L^{-1}	8.0 μg L^{-1}	41
Time resolved fluorometry	Sandwich immunoassay	Lanthanide ions labels	0–1000 μg L^{-1}	2.0 μg mL^{-1}	42
Laser induced fluorescence	Sandwich immunoassay	-Silica Nanoparticles as immobilization support	0–580 ng mL^{-1}	0.87 ng mL^{-1}	39
Amperometry	Sandwich immunoassay	-Copper Nanoparticlesas electrode modification -Magnetic Nanoparticles as immobilization support	0–580 ng mL^{-1}	1.1 ng mL^{-1}	PM

PM = presented method

The accuracy of the method was evaluated with a dilution test, it was performed using a 580 ng mL^{-1} IRT sample that was serially diluted in PBS (0.01 M, pH 7.2). The assays on the dilutions maintained a linear response, with a correlation coefficient $r = 0.997$.

In this work, three IRT high level neonatal samples, three IRT high level control samples (provided with the Trypsin MW ELISA Kit) and five low level neonatal samples were analyzed. All samples were previously confirmed for IRT using the commercial Trypsin MW ELISA Kit. High level samples and controls were later analyzed by our quantitative method, which revealed high concentrations of IRT in all of them. The low level samples showed also low concentrations by our method.

Moreover, the method was compared with a commercial ELISA procedure for the quantification of IRT. Both response signals show a correlation close to 1, indicating a good correspondence between the two methods (Fig. 4).

The LOD is the concentration that gives a signal 3 times the standard deviation ofthe blank. For the immunosensor and the ELISA test kit, the LODs were 1,1 ng mL^{-1} and 4.2 ng mL^{-1}, respectively. Thus, the sensor significantly enhances the detection limit.

The total assay time required for the IRT determination employing Blood Spot Trypsin-MW ELISA Kit was approximately 12 h, including the extraction procedure. In contrast, the ultrasonic sample elution preparation and the IRT determination by the immunosensor requires a total assay time of <40 min.

According to our detailed search, few previously reported articles related to IRT detection were published. It is important to highlight that our method is the only electrochemical microfluidic immunosensor reported to date, while the remaining articles used LIF as detection system. Xu et al. showed an assay based on immunoreagents labeled with lanthanide ions, on dissociative fluorescence enhancement applying the principle of co-fluorescence, and on time-resolved fluorometry [41]. Lindau-Shepard et al. developed a multiplex immunoassay using two different Luminex bead sets for IRT isoforms detection [42]. Seia et al. [39] developed a microfluidic device, coupled to LIF detection, with 3-aminopropyl functionalized silica nanoparticles-APTES biorecognition platform. It is relevant to emphasize that our method is based on microfluidic technology, using CuNPs-AuE for the electrochemical detection. MNPs were used as biorecognition platform, which allowed the successfully immobilization of anti-IRT-monoclonal Ab as a strategy to provide specificity to the device. In addition, the achieved LOD was lower than that obtained by the above mentioned articles [40, 41] (Table 3).

Considering the CF neonatal screening cut off value, all obtained LODs were reasonably good. Finally, our device presents inherent benefits such as miniaturization, integration, portability and the possibility to perform on-site analysis.

Conclusion

In this article, we describe a microfluidic immunosensor with electrochemical detection for the quantitative determination of IRT as marker for CF diagnosis. The sensor combines the microfluidic technology, the sensitivity of the electrochemical detection and the immunoassay specificity. These features allowed us to obtain a sensitive and selective device with portability and lower power requirements. Moreover, the incorporation of MNPs as a bioaffinity support and the electrodeposition of CuNPs increase the active area and improve of the sensitivity respectively. Compared with the conventional ELISA analysis, our immunosensor reduces the total assay time, with our sensor it was less than 40 min.

In summary, an alternative analytical method for CF newborn screening was developed. The microfluidic immunosensor displays excellent analytical performance for the selective and sensitive IRT determination.

Acknowledgments The authors wish to thank the financial support from the Universidad Nacional de San Luis (UNSL), the Instituto de Química de San Luis (INQUISAL), the Consejo Nacional de Investigaciones Científicas y Técnicas (CONICET) and the Agencia Nacional de Promoción Científica y Tecnológica (ANPCyT).

References

1. Kerem B, Rommens J, Buchanan J, Markiewicz D, Cox T, Chakravarti A, et al (1989) Identification of the cystic fibrosis gene: genetic analysis. Science 245:1073–1080

2. Soave D, Miller M, Keenan K, Li W, Gong J, Ip W, et al (2014) Evidence for a causal relationship between early exocrine pancreatic disease and cystic fibrosis-related diabetes: a mendelian randomization study. Diabetes 63:2114–2119
3. Minasian C, McCullagh A, Bush A (2005) Cystic fibrosis in neonates and infants. Early Hum Dev 81:997–1004
4. Farrell PM (2008) Is newborn screening for cystic fibrosis a basic human right? J Cyst Fibros 7:262–265
5. Castellani C, Southern KW, Brownlee K, Dankert Roelse J, Duff A, Farrell M, et al (2009) European best practice guidelines for cystic fibrosis neonatal screening. J Cyst Fibros 8:153–173
6. Miller MR, Soave D, Li W, Gong J, Pace RG, Boëlle P, Cutting GR, Drumm ML, Knowles MR, Sun L, Rommens JM, Accurso F, Durie PR, Corvol H, Levy H, Sontag MK, Strug LJ (2015) Variants in solute carrier SLC26A9 modify prenatal exocrine pancreatic damage in cystic fibrosis. J Pediatr 166(5):1152–1157
7. Therrell Jr BL, Hannon WH, Hoffman G, Ojodu J, Farrell PM (2012) Immunoreactive trypsinogen (IRT) as a biomarker for cystic fibrosis: challenges in newborn dried blood spot screening. Mol Genet Metab 106:1–6
8. Sommerburg O, Krulisova V, Hammermann J, Lindner M, Stahl NM, Muckenthaler M, Kohlmueller D, Happich M, Kulozik AE, Votava F, Balascakova M, Skalicka V, Stopsack M, Gahr M, Macek Jr M, Mall MA, Hoffmann GF (2014) Comparison of different IRT–PAP protocols to screen newborns for cystic fibrosis in three central European populations. J Cyst Fibros 13:15–23
9. DiBattista A, Macedo AN, Al-Dirbashi OY, Chakraborty P, Britz-McKibbin P (2014) Metabolomics for discovery of biomarkers for cystic fibrosis: towards MS-based primary screening methods with improved positive predictive value. Clin Biochem 47(15):143
10. Kim NH, Jeong JS, Kwon HJ, Lee YM, Yoon HR, Lee KR, Hong SP (2010) Simultaneous diagnostic method for phenylketonuria and galactosemia from dried blood spots using high-performance liquid chromatography-pulsed amperometric detection. J Chromatogr B 878:1860–1864
11. Mo X, Li Y, Tang A, Ren Y (2013) Simultaneous determination of phenylalanine and tyrosine in peripheral capillary blood by HPLC with ultraviolet detection. Clin Biochem 46:1074–1078
12. Chuang W, Pacheco J, Zhang XK, Martin MM, Biski CK, Keutzer JM, Wenger DA, Caggana M, Orsini Jr JJ (2013) Determination of psychosine concentration in dried blood spots from newborns that were identified via newborn screening to be at risk for krabbe disease. Clin Chim Acta 419:73–76
13. Tang J, Tang DP, Su BL, Li QF, Qiu B, Chen GN (2011) Silver nanowire-graphene hybrid nanocomposites as label for sensitive electrochemical immunoassay of alpha-fetoprotein. Electrochim Acta 56:8168–8175
14. Wang J (2002) Portable electrochemical systems. Trends Anal Chem 21:226–232
15. Bange A, Halsall HB, Heineman WR (2005) Microfluidic immunosensor systems. Biosens Bioelectron 20:2488–2503
16. Pumera M, Merkoci A, Alegret S (2006) New materials for electrochemical sensing VII. Microfluidic chip platforms. Trends Anal Chem 25:219–235
17. Tang J, Tang D (2015) Non-enzymatic electrochemical immunoassay using noble metal nanoparticles. Microchim Acta 182(13): 2077–2089
18. Lohse SE, Murphy CJ (2012) Applications of colloidal inorganic nanoparticles: from medicine to energy. J Am Chem Soc 134: 15607–15620
19. Zhu Z, Shi L, Feng H, Zhou HS (2015) Single domain antibody coated gold nanoparticles as enhancer for Clostridium difficile toxin detection by electrochemical impedance immunosensors. Bioelectrochemistry 101:153–158
20. Yang Z, Liu Y, Lei C, Sun X, Zhou Y, (2015) A flexible giant magnetoimpedance-based biosensor for the determination of the biomarker C-reactive protein Microchimica Acta doi:10.1007/s00604-015-1587-4
21. Ding L, Bond AM, Zhai J, Zhang J (2013) Utilization of nanoparticle labels for signal amplification in ultrasensitive electrochemical affinity biosensors: a review. Anal Chim Acta 797:1–12
22. Pumera M, Escarpa A (2009) Nanomaterials as electrochemical detectors in microfluidics and CE: fundamentals, designs, and applications. Electrophoresis 30:3315–3323
23. Zhao D, Xu BQ (2006) Enhancement of Pt utilization in electrocatalysts by using gold nanoparticles. Angew Chem Int Ed Engl 45:4955–4959
24. Yang R, Qiu X, Zhang H, Li J, Zhu W, Wang Z, Huang X, Chen L (2005) Monodispersed hard carbon spherules as a catalyst support for the electrooxidation of methanol. Carbon 43:11–16
25. Boo H, Park S, Ku B, Kim Y, Park JH, Kim HC, Chung TD (2004) Ionic strength-controlled virtual area of mesoporous platinum electrode. J Am Chem Soc 126:4524–4525
26. Papadimitriou S, Tegou A, Pavlidou E, Kokkinidis G, Sotiropoulos S (2007) Methanol oxidation at platinised lead coatings prepared by a two-step electroless deposition-electrodeposition process on glassy carbon substrates. Electrochim Acta 52:6254–6260
27. Salimi A, Hallaj R, Soltanian S, Mamkhezri H (2007) Nanomolar detection of hydrogen peroxide on glassy carbon electrode modified with electrodeposited cobalt oxide nanoparticles. Anal Chim Acta 594:24–31
28. Jiang Y, Lu Y, Li F, Wu T, Niu L, Chen W (2012) Facile electrochemical codeposition of clean graphene–Pd nanocomposite as an anode catalyst for formic acid electrooxidation. Electrochem Commun 19:21–24
29. Kun Z, Ling Z, Yi H, Ying C, Dongmei T, Shuliang Z, Yuyang Z (2012) Electrochemical behavior of folic acid in neutral solution on the modified glassy carbon electrode: platinum nanoparticles doped multi-walled carbon nanotubes with nafion as adhesive. J Electroanal Chem 677–680:105–112
30. Nantaphol S, Chailapakul O, Siangproh W (2015) Sensitive and selective electrochemical sensor using silver nanoparticles modified glassy carbon electrode for determination of cholesterol in bovine serum. Sensors Actuators B Chem 207:193–198
31. Lin X, Ni Y, Kokot S (2013) Glassy carbon electrodes modified with gold nanoparticles for the simultaneous determination of three food antioxidants. Anal Chim Acta 765:54–62
32. Goel S, Chen F, Cai W (2014) Synthesis and biomedical applications of copper sulfide nanoparticles: from sensors to theranostics. Small 10:631–645
33. Guo M, Wang P, Zhou C, Xia Y, Huang W, Li Z (2014) An ultrasensitive non-enzymatic amperometric glucose sensor based on a Cu-coated nanoporous gold film involving co-mediating. Sensors Actuators B Chem 203:388–395
34. Karlsson HL, Cronholm P, Gustafsson J, Möller L (2008) Copper oxide nanoparticles are highly toxic: a comparison between metal oxide nanoparticles and carbon nanotubes. Chem Res Toxicol 21: 1726–1732
35. Kumar SA, Cheng H-W, Chen S-M, Wang S-F (2010) Preparation and characterization of copper nanoparticles/zinc oxide composite modified electrode and its application to glucose sensing. Mater Sci Eng C 30:86–91
36. Biomedicals MP (2011) ImmunoChem blood spot trypsin-MW ELISA kit, MP Biomedicals
37. Segato TP, Coltro WK, Almeida AL, Piazetta MH, Gobbi AL, Mazo LH, Carrilho E (2010) A rapid and reliable bonding process for microchip electrophoresis fabricated in glass substrates. Electrophoresis 31:2526–2533
38. Fischer LM, Tenje M, Heiskanen AR, Masuda N, Castillo J, Bentien A, Émneus J, Jakobsen MH, Boisen A (2009) Gold cleaning methods for electrochemical detection applications. Microelectron Eng 86:1282–1285

39. Seia MA, Stege PW, Pereira SV, De Vito IE, Raba J, Messina GA (2014) Silica nanoparticle-based microfluidic immunosensor with laser-induced fluorescence detection for the quantification of immunoreactive trypsin. Anal Biochem 463:31–37
40. Liu GD, Yan JT, Shen GL, Yu RQ (2001) Renewable amperometric immunosensor for complement 3 (C3) assay in human serum. Sensors Actuators B Chem 80:95–100
41. Xu YY, Pettersson K, Blomberg K, Hemmilä I, Mikola H, Lövgren T (1992) Simultaneous quadruple-label fluorometric immunoassay of thyroid-stimulating hormone, 17 alpha-hydroxyprogesterone, immunoreactive trypsin, and creatine kinase MM isoenzyme in dried blood spots. Clin Chem 38:2038–2043
42. Lindau Shepard AB, Pass KA (2010) Newborn screening for cystic fibrosis by use of a multiplex immunoassay. Clin Chem 56:445–450